Journal of Ocean, Mechanical and Aerospace
-Science and Engineering-, Vol.42

April 30, 2017

New Engine Simulation Structure Model Applied to SI Engine

Mohammad Javad Nekooei,[a] and J.Koto,[a,b,*]

[a)]*Faculty of Mechanical Engineering, Universiti Teknologi Malaysia, Malaysia.*
[b)]*Ocean & Aerospace Research Institute, Indonesia*

*Corresponding author: jaswar.koto@gmail.com and jaswar@utm.my.

Paper History

Received: 1-March-2017
Received in revised form: 28-April- 2017
Accepted: 30-April- 2017

ABSTRACT

High ratio emissions that outcome from incomplete combustion cause air contamination, poorer the performance of the spark ignition (SI) engine and raise fuel consumption. Uncompleted combustion emitted a high ratio of CO, HC, NO_x and PM harmful emissions such as come into atmosphere. This study has reviewed existing engine simulation structures using different methods as s as follows Neural Networks (NN), Sliding Mode Control (SMC), Proportional–Integral (PI) Predictive Control (MPC) and DRNN-based MPC method. The existing engine models were compared with the new engine simulation structure model which was proposed by the authors, using Hybrid Fuzzy Logic Control (HFLC) method in term of AFR. The simulation engine model in Matlab/Simulink using new engine simulation has founded that AFR (15.02, 14.4) which closes to the stoichiometric value of 14.7 compared by using Neural Networks (NN) method, a Sliding Mode Control (SMC) method, a Proportional–Integral (PI) control method, Model Predictive Control (MPC) method and DRNN-based MPC method.

KEY WORDS: *New Engine Simulation Structure, SI Engine; Structure Model; Emission*

NOMENCLATURE

AFR	Air to Fuel Ratio
DRNN	Diagonal Recurrent Neural Network
EGR	Exhaust Gas Recirculation
MEP	Mean Effective Pressure
MPC	Model Predictive Control
MVEM	Mean Value Engine Model
NN	Neural Networks,
PI	Proportional–Integral
RBF	Radial Basis Function
RLS	Recursive Least-Squares
P_i	Pressure of intake manifold
n	Speed of engine
m_f	Flow rate of fuel to the intake valve
T_i	Temperature of intake air
m_{at}	Air mass flow past throttle plate
m_{ap}	Air mass flow into the intake port

1.0 BACKGROUND OF ENGINE SIMULATION MODELS

Environment in forms of air pollution emitted by land, ocean and air transportation systems such as hydrocarbons (HC), compounds of hydrogen nitrogen (NO_x), carbon dioxide (CO_2), particulate matter (PM) and sulfur oxides (SO_x),) became an essential issue on societies' point of view. The eco-fuel and clean emissions are more stringent legislation, improvements in engine control transient performance emerged as an important issue. The Kyoto Protocol (1997) has been a turning point for the future economic and environmental policies for both industrialized and developing countries [Koto, et.al, 2002].

An internal combustion (IC) engine in a vehicle needs to operate smoothly, from idle to high speeds, and under varying inertial loads, disturbances and throttle settings. In addition, the industry is faced with meeting stringent fuel consumption and emissions regulations [Pieper, et.al, 1999]. Tail-pipe emissions

JOMAse | Received: xxx | Accepted: xxx | [(42) 1: 1-18]
Published by International Society of Ocean, Mechanical and Aerospace Scientists and Engineers, www.isomase.org., ISSN: 2354-7065 & e-ISSN: 2527-6085

reductions using a three-way catalytic converter can be done by controlling the ratio of air-to-fuel (AFR) with very precisely in the steady state operation and transient engine, Mean AFR variation: $\pm 0.2\%$ [Benninger, et.al, 1991].

Figure 1 shows an engine management systems typically consist of an engine control unit and a common core of sensors and actuators. The principal engine sensors include crank position/engine speed, manifold absolute pressure or airflow sensor, throttle position, coolant temperature, and exhaust gas oxygen (O_2), while the principal engine actuators include the fuel injectors and electronic spark [Bosch, 1994] & [Wagner, et.al, 2003].

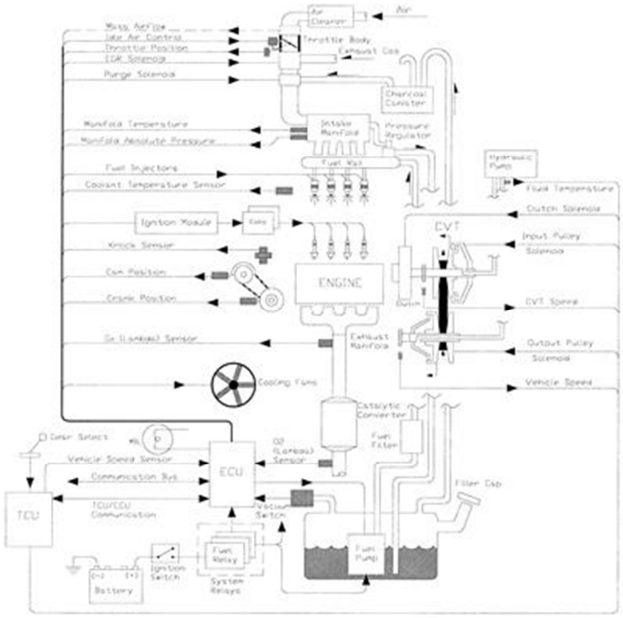

Figure 1: Engine management system [Wagner, et.al, 2003].

Late at 1970's, a model which is produced by [Cassidy, et.al, 1980] has been generally settled as a standout amongst the most widely recognized routines for the depiction of engine systems (SYS). Four fundamental segments of the SYS are incorporated in this model. They are exhaust gas recirculation (EGR), fuel, intake and ignition SYSs. Cassidy model give well execution in simulating procedure, be that as it may, because of its inconvenience, it is not proper for development and assessment of the engine control SYSs. Aftereffects of reenactment and tests are the premise of the model and it has a restricted notoriety. Linearization is utilized for acquiring a percentage of the mathematical statements and parameters of the model so that the dynamic attributes of engine can't be accurately reflected. From 1980s to now, the electronic controlled engine utilized both of static engine model and the semi static engine model [Hendricks, et.al, 1991 & 1996], [Nekooei, et.al, 2013, 2014 & 2015], [Priyanto, et.al, 2014], [Cassidy, et.al, 1980].

It is conceivable to mirror a few engine presentation parameters in the stable conditions because of steady state examinations of engine are the source of model information. Two fundamental purposes behind putting these models separated and not utilizing them prevalently are:

They can't mirror the dynamic attributes while the engine is working under transient conditions. They are absolutely needy to the experimental information so that require high measure of labour and material resources. For conquering the disadvantages of the aforementioned engine models and simulation of the qualities of dynamic, a model named the mean value engine model (MVEM) was arranged and got extra advancement by distinctive researchers [Balluchi, et.al, 1999].

Finally, Hendricks methodically compressed the mean model [Cassidy, et.al, 1980]. For the most part, for explaining the dynamic procedure of the engine, the mean value of variables included in cycle SYS of the engine is utilized as a part of this model. Accordingly, the engine dynamic qualities can be effectively reflected in the transient conditions. In this manner, researchers and analysts created and upgraded the MVEM overwhelmingly in the oil film are and in addition the torque models. Together with the science and innovation change, numerous researchers improved the MVEM; they have connected hybrid models and astute control also. The extent of the MVEM application has been spread by [Cook, et.al, 1988] since he connected this model to a turbocharged gas engine. The air/fuel effect and spark angle have been considered by [Nekooei, et.al 2013] on the yield torque. Subsequently, by a low precision model mistake of beneath 5%, it is conceivable to apply the mean model to the lean burn engine. For displaying of gasoline engine, a hybrid model was set up by [Alippi, et.al, 1988 & 2003].

2.0 EXISTING ENGINE SIMULATION STRUCTURE

A few diverse simulation model structures are exist that are excluded in this writing survey. This is on account of they may be like the examined models or lack adequate points of interest. In 1988, Cook and Powel studied non-thermodynamic modeling of automotive internal combustion engines and show how adequate linear model can be developed for the analysis of control. The nonlinear engine simulation model contains representations of the throttle body, engine pumping phenomena, induction process dynamics, fuel system, engine torque generation, and rotating inertia as shown in Figure 2 [Cook, et.al, 1988]. The engine structure consists of throttle body, manifold plenum, engine pump, fuel system and engine power and inertia.

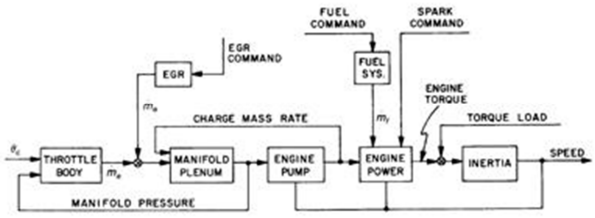

Figure 2: Nonlinear Engine Model [Cook, et.al, 1988]

The linearized version of the engine model is illustrated in Figure.3. According to the figures, it was founded that there is no thermodynamic model included in their study for car IC engines. Be that as it may, the throttle dynamics, pumping wonders of engine, prompting procedure dynamics, SYS of fuel injection,

JOMAse | Received: xxx | Accepted: xxx | [(42) 1: 1-18]
Published by International Society of Ocean, Mechanical and Aerospace Scientists and Engineers, www.isomase.org., ISSN: 2354-7065 & e-ISSN: 2527-6085

torque of engine, inertia of rotating and EGR SYS dynamics are being spoken to in this simulation model.

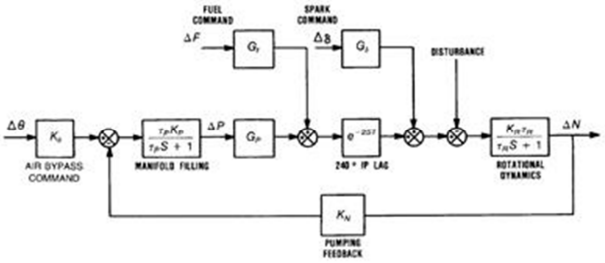

Figure 3: Block diagram of linear Engine Model [Cook, et.al, 1988].

In 1999, Pieper and Mehrotra studied a sliding mode controller for the linear and nonlinear models. Fuel injected SI engine model was developed including intake manifold, fuel wall-wetting and crankshaft dynamics as well as load effects and process delays inherent in four-stroke engines. A sliding mode controller is designed and implemented for a linearized model using state estimates [Alippi, et.al, 1988, & 2003]. Priyanto, et.al 2014 also designed online artificial gain updating sliding mode Algorithm and has applied to internal combustion engine [Priyanto, et.al, 2014]

Countless of SI engines can be simulated by an engine model which a nonlinear dynamic model studied by Yoon.et.al in 2000. He introduced nonlinear dynamic models of engine as shown Figure 4, that can be applied to various kinds of operations of SI engines in which the dynamic model using test data from both the stable operation and transient and nonlinear estimation techniques [Wang, et.al, 2006 & 2008]. The engine structure consists of throttle body, intake manifold dynamics, fuel film dynamics, rotational engine dynamic, lambda, delay sensor dynamic and torque production modules. In order for the development of the proposed engine model, he used 2.0L, an inline 4 cylinder DOHC engine and an eddy current type dynamometer.

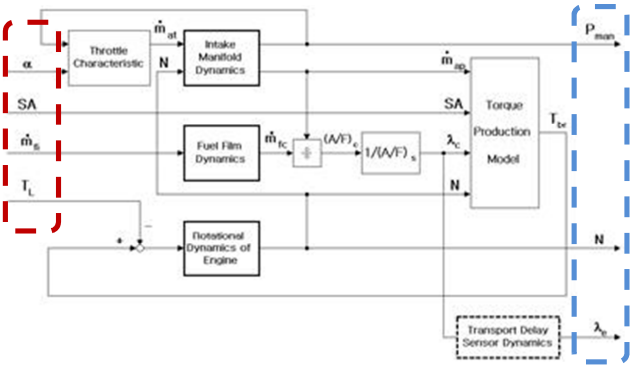

Figure 4: Nonlinear Dynamic Engine Model [Yoon, et.al, 2000]

Diverse variables which are incorporated in the engine simulation model are represented as follows:

The input variables (red break line) are as follows:

- angle of throttle (α) for throttle body,
- flow rate of fuel ($\dot{m}_{fi}$) for fuel film dynamics,
- spark timing (SA) for torque production,

Disturbance:

- load of torque (T_L) for rotational engine dynamics,

State variables:

- mass of air in throttle ($\dot{m}_{at}$) from throttle body to intake manifold dynamic,
- mass of air into cylinder ($\dot{m}_{ap}$) from intake manifold to torque production,
- air to fuel ratio (λ_c from AFR to torque production,
- engine brake torque (T_{br}) from torque production to rotational engine dynamic
- mass of fuel in the fuel film (m_{fc}) from fuel film dynamic

The output variables (blue break line) are as follows:

- pressure of intake manifold (P_{man}) from intake manifold dynamics,
- speed of engine (N)
- AFR time delay (λ_e) from delay sensor dynamic.

Mass of air and fuel into the cylinder is initially calculated by the model. Besides, the engine AFR is processed. Figure 4.a shows the intake manifold dynamic structure. At long last, for calculating torque of the engine brake, torque generation model is used. The Schematic diagram of torque production model is shown in Figure 4.b. Rotational dynamics of the engine, intake manifold and fuel film are incorporated in the model of and transport delays which are common in the four stroke engine cycles [Yoon, et.al, 2000].

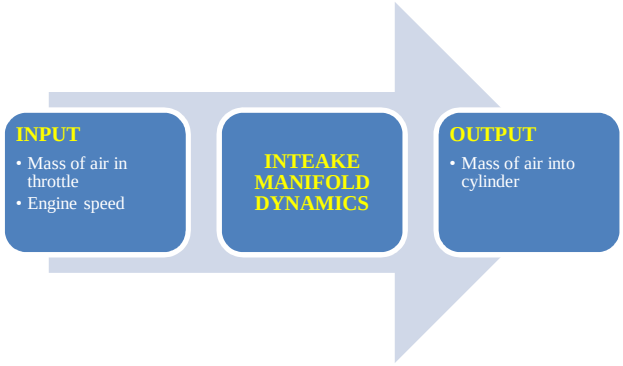

Figure 4.a: Intake manifold dynamic structure.

Based the study Yoon.et.al concluded that the simulation data from the model shows a good agreement with the measured data during the engine test. Their claimed that the nonlinear engine model is mathematically compact enough to run in real time, and can be used as an embedded model within a control algorithm or an observer when a powertrain controller is designed and developed.

JOMAse | Received: xxx | Accepted: xxx | [(42) 1: 1-18]
Published by International Society of Ocean, Mechanical and Aerospace Scientists and Engineers, www.isomase.org., ISSN: 2354-7065 & e-ISSN: 2527-6085

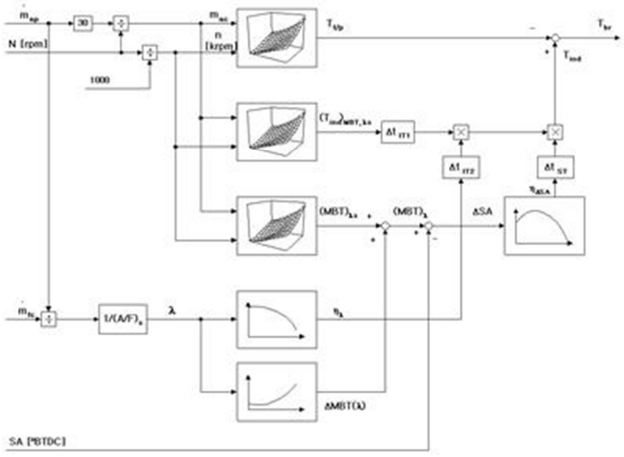

Figure 4.b: Schematic diagram of torque production model [Yoon, et.al, 2000].

Alippi.et.al, 1998 presented an application of neural techniques in the automotive field the control of AF to keep minimum value the exhaust car engine emissions. In the study, the neural controller had been obtained with an indirect control scheme, based on a neural model of the process: it was designed to optimize performance and limit the necessary control actions [Alippi, et.al, 1988 & 2003].

Figure 5.a outlines the structure of engine simulation structure proposed by Alippi.et.al, 1998 which has some crucial and fundamental constituting blocks. The engine structure consists of manifold dynamic, cylinder air intake, fuel film deposition dynamic (wall wetting) and AFR modules.

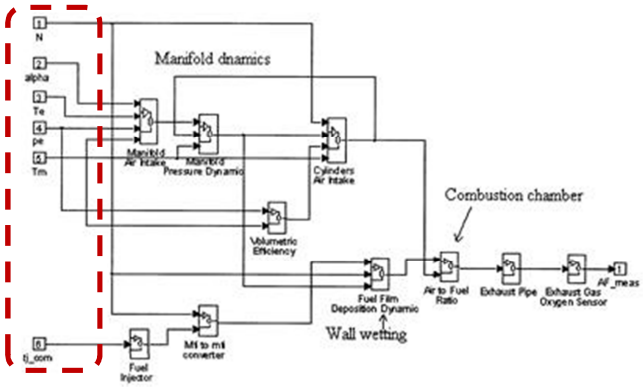

Figure 5.a: Engine Simulation Block [Alippi, et.al, 1988 & 2003]

According to the Figure 5.a, there are six engine model inputs (red break line) as follows:

- Speed of engine (N) for cylinder air intake and converter,
- Angle of the throttle (α) for manifold air intake,
- External temperature (T_e) for manifold air intake,
- External pressure (P_e) for manifold air intake,
- Temperature of engine manifold (T_m) for manifold pressure and cylinder air intake,
- Time of fuel injection (T_f) for fuel injector.

A block description of the training configuration is given in Figure.5.b, where $\overline{AF} = 14.64$ is the stoichiometric value for AF [Alippi, et.al, 1988 & 2003]. This control scheme is quite flexible and allows the network for subsequent online training.

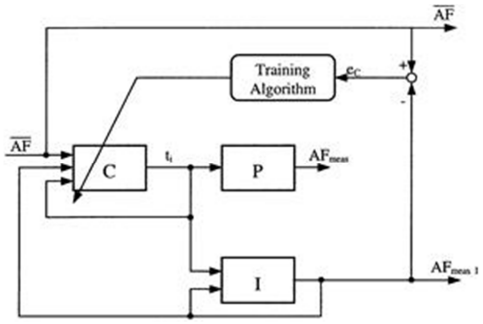

Figure 5.b: Training configuration for the neural controller [Alippi, et.al, 1988 & 2003].

The AFR can be spoken to by the simulation block output. Really, by method for gathering the block of manifold air intake, dynamic of manifold pressure and block of cylinder air intake, it is conceivable to perform the estimations of the air mass into the cylinder. Measure of fuel mass into the cylinder can be dictated by utilizing fuel injector and the dynamic of fuel film deposition, utilizing a proper physical driven model, two blocks. Identification with the AFR and exhaust pipe are characterized as engine AFR.

In 2003, Alippi.et.al also studied on a neural based solution to the air-to-fuel ratio control in fuel injection systems. They introduced an indirect control approach which required a preliminary modeling of the engine dynamics. The engine model and the final controller were based on recurrent neural networks with external feedbacks. They had integrated requirements for feasible control actions and the static precision of control in the controller design to guide learning toward an effective control solution.

Wang et.al, 2006, the model predictive control (MPC) based on a neural network model is attempted for air-fuel ratio, in which the model is adapted on-line to cope with nonlinear dynamics and parameter uncertainties. A radial basis function (RBF) network as shown in Figure 6.d, is employed and the recursive least-squares (RLS) algorithm is used for weight updating. The engine structure consists of manifold pressure and temperature, fuel injection, AFR engine speed and time delay modules. The engine simulation model used in this study is an expanded system based on the generic mean value engine model developed by Hendricks, et.al as shown in Figure 6.a [Wang, et.al, 2006 & 2008].

JOMAse | Received: xxx | Accepted: xxx | [(42) 1: 1-18]
Published by International Society of Ocean, Mechanical and Aerospace Scientists and Engineers, www.isomase.org., ISSN: 2354-7065 & e-ISSN: 2527-6085

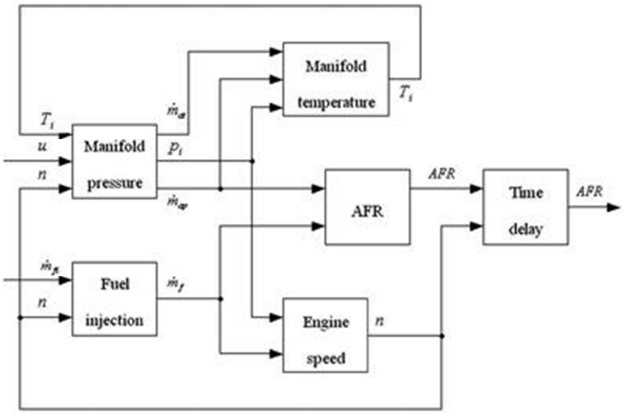

Figure 6.a: Engine Simulation Model [Wang, et.al, 2006 & 2008, Zhai, et.al, 2008, 2009 & 2011]

Figure 6.a demonstrates the model of engine simulation which is introduced by Wang et.al. The DRNN model is made adaptive on- line to deal with engine time varying dynamics, so that the robustness in control performance is greatly enhanced. There are two input variables for fuel injection structure as follows: throttle open angle (u) and fuel flow rate (m_{fi}), and one output (AFR) as shown in Figure 6.b. Symbols utilized as a part of this model are as per the following:

- Pressure of intake manifold (P_i) from manifold pressure to manifold temperature and engine speed.
- Speed of engine (n)
- Flow rate of fuel to the intake valve ($\dot{m}_f$) from fuel injection to AFR and engine speed.
- Temperature of intake air (T_i) from manifold temperature to manifold pressure
- Air mass flow past throttle plate ($\dot{m}_a$) from manifold pressure to manifold temperature
- Air mass flow into the intake port ($\dot{m}_{ap}$) from manifold pressure to AFR

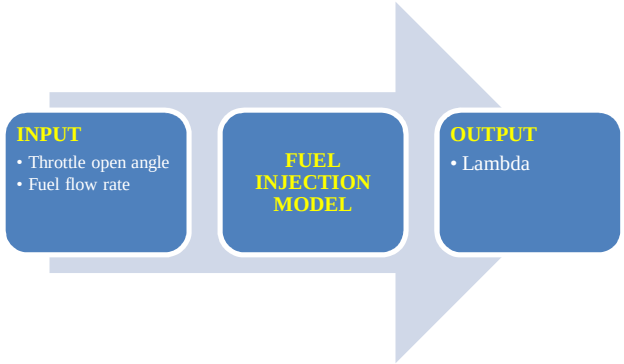

Figure 6.b: Fuel injection structure

By executing air mass flow and fuel into the intake port which is taken structure manifold pressure block and fuel injection block, the AFR is calculated in the AFR block. Figure 6.c shows the AFR structure with inputs such as air mass flow into the intake port ($\dot{m}_{ap}$) and flow rate of fuel to the intake valve ($\dot{m}_f$).

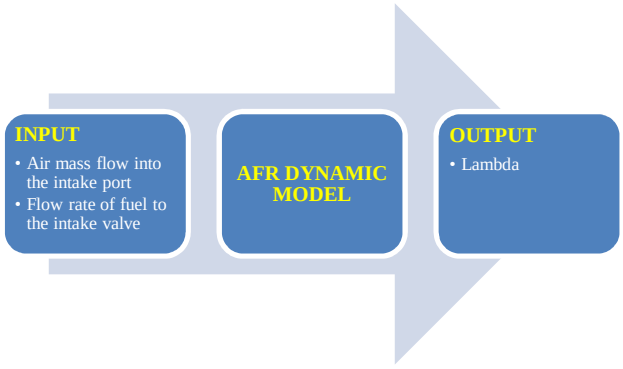

Figure 6.c: AFR structure

The strategy of MPC for SI engines is shown in Figure 6.d. The RBF neural network has three layers: the input layer, the hidden layer and the output layer. The hidden layer consists of an array of computing units called hidden nodes. The strategy of MPC for SI engines is shown in Figure 6.d. The obtained adaptive RBF neural network is used to predict the engine output for N_2 steps ahead.

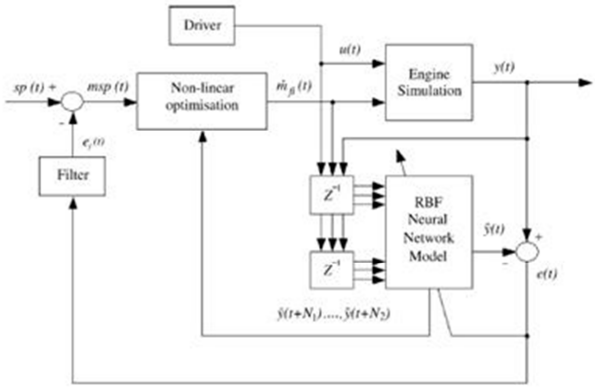

Figure 6.d: The adaptive neural network model-based predictive control strategy [Wang, et.al, 2006 & 2008]

Using the same engine model as previous work, Wang et.al, 2008 introduced an adaptive neural network method to estimate two immeasurable physical parameters on-line and to compensate for the model uncertainty and engine time varying dynamics. Using the method the chattering was substantially reduced and the air–fuel ratio is regulated within the desired range of the stoichiometric value. In the study, the adaptive law of the neural network was derived using the Lyapunov method to reassure the stability of the whole system and the convergence of the networks. The overall system configuration of the DSMC scheme with RBF network adaptation including the neural network estimators is shown in Figure 6.f.

JOMAse | Received: xxx | Accepted: xxx | [(42) 1: 1-18]
Published by International Society of Ocean, Mechanical and Aerospace Scientists and Engineers, www.isomase.org., ISSN: 2354-7065 & e-ISSN: 2527-6085

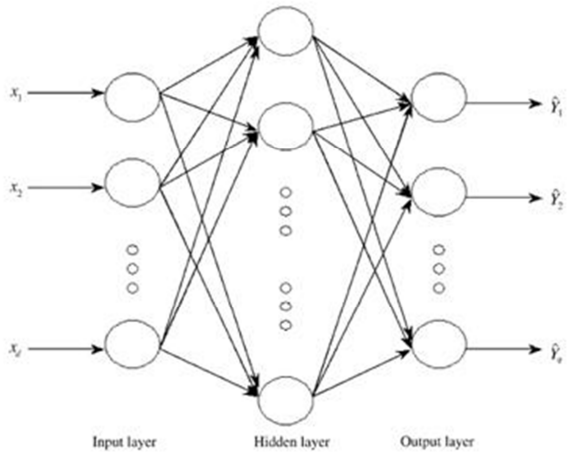

Figure 6.e: The RBF neural network structure [Wang, et.al, 2006 & 2008]

In like manner, in the block of speed of engine, the engine speed is computed. Block of time delay is utilized for simulating the AFR time delay which is join in the counts amid the simulation of engine. Model of manifold temperature alludes to the air mass flow into the intake port, intake manifold pressure and air mass flow past throttle plate for processing the intake manifold temperature. Dynamics of Fuel film of the intake ports can be simulated by the fuel injection model.

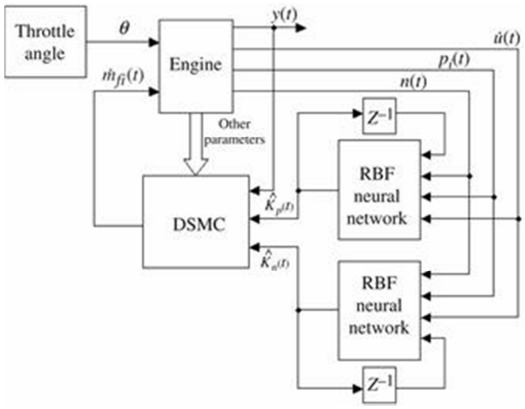

Figure 6.f: The DSMC scheme with on-line parameter adaptation [Wang, et.al, 2006 & 2008].

Zhai, et.al, 2009 applied the model predictive control (MPC) strategy to engine air/fuel ratio control using neural network model using the same engine model as Wang, et.al in 2006 & 2008. The neural network model uses information from multi-variables and considers engine dynamics to do multi-step ahead prediction. The model is adapted in on-line mode to cope with system uncertainty and time varying effects. Thus, the control performance is more accurate and robust compared with non-adaptive model based methods. They developed a non-linear model predictive control scheme for AFR based on a radial basis function (RBF) neural network model as shown in Figure 7.a.

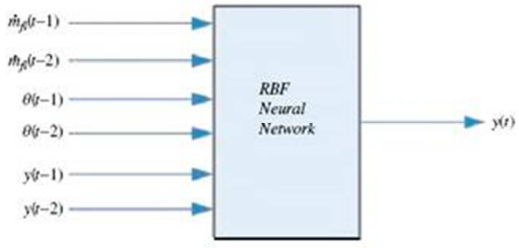

Figure 7.a: RBF model structure [Yoon, et.al, 2000].

In 2010, using the same engine simulation model as Wang, et.al, Zhai, et.al, 2010 also investigated engine modeling with the Diagonal Recurrent Neural Network (DRNN) and such a model-based predictive control for AFR. In order to obtain the engine data for DRNN modelling, two sets of random amplitude signal (RAS) were designed for throttle angle (θ) and fuel injection rate (m_{fi}) as shown in Figure 7.b.

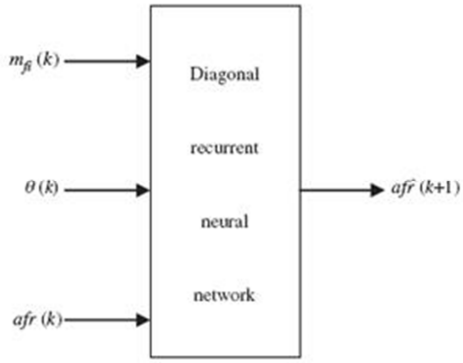

Figure 7.b: The DRNN model input [Zhai, et.al, 2010].

Zhai, et.al 2011 had development of fast modern computers to extend model predictive control (MPC) method to automotive engine control systems, which is traditionally applied to plants with dynamics slow enough to allow computations between samples. They attempted MPC based on an adaptive neural network model for air fuel ratio (AFR), in which the model was adapted on-line to cope with nonlinear dynamics and parameter uncertainties. A radial basis function (RBF) network was employed and the recursive least squares (RLS) algorithm is used for weight updating [Zhai, et.al].

In 2013, Yang Bai, introduced an engine simulation structure as shown in Figure 7.a. From Figure 7.a, the engine structure orderly consists of seventh major modules for the engine operation as follows:

1. Throttle body model
2. Intake manifold dynamic model
3. Fuel injection dynamic model
4. Wall wetting dynamic model
5. Lambda dynamic model
6. Crank shaft rotational dynamic model
7. Torque production dynamic model

JOMAse | Received: xxx | Accepted: xxx | [(42) 1: 1-18]
Published by International Society of Ocean, Mechanical and Aerospace Scientists and Engineers, www.isomase.org., ISSN: 2354-7065 & e-ISSN: 2527-6085

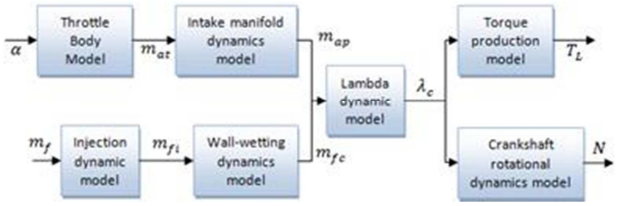

Figure 7.a: Engine simulation system signal flow graph where: throttle open angle (α), air mass in throttle (mat), air mass into cylinder (map), AFR (λ_c), torque output (T_L), fuel flow rate (m_f), fuel mass injected (m_{fi}), fuel mass into cylinder (m_{fc}), engine speed (N) by Yang Bai, 2013 [Bai, 2014].

From operation structure, the engine system can be divided into three parts: air flow system, fuel flow system and torque generation system as shown in Figure 7.b. The engine operation is divided into five major mathematical modules which are: throttle body model, intake manifold dynamic model, fuel delivery model, torque production model and engine rotational dynamics model. The fuel delivery simulation model has been separated into two parts: injection dynamics and wall-wetting dynamics as shown in Figure 7.c.

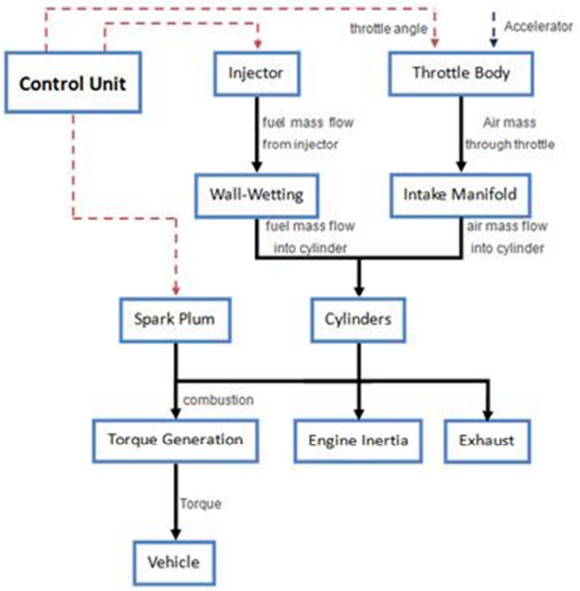

Figure 7.b: Engine operation structure by Yang Bai, 2014.

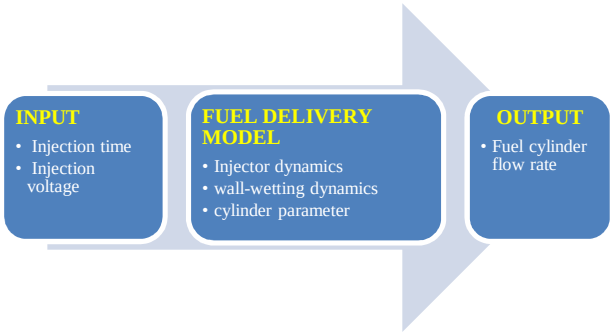

Figure 7.c: Fuel delivery structure model by Yang Bai, 2013

A fuzzy PID control has used to control air/fuel ratio in Spark-ignition engines to maximize the fuel economy while minimizing exhaust emissions. Inverse control and predictive control was trained offline as shown in Figure 7.d in which the control output was modified to compensate control error [Bai, 2014]. Experiment using 4G64 Mitsubishi engine had been conducted to validate the simulation model.

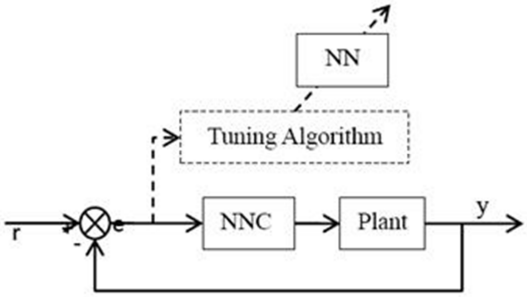

Figure 7.d: NN Controller Tuning Schematic by Yang Bai, 2013 [37].

3.0 NEW ENGINE SIMULATION STRUCTURE

This study was continuation from previous studies on engine structure models and control system. They are as follows: designing fuzzy back-stepping adaptive based fuzzy estimator variable structure control: applied to internal combustion engine in 3013 [Nekooei, et.al, 2013], combustion control of marine engine by fuzzy logic control concerning the air to Fuel Ratio in 2014 [Nekooei, et.al], simple fuzzy logic diagnosis system for control of internal combustion engines in 2015 [Nekooei, et.al, 2015], combustion modelling of marine spark-ignition engines in 2015 [Nekooei, et.al, 2015] and a and a new engine simulation Structure model applied to SI engine controlling in 2015 [Nekooei, et.al, 2015].

In the previous study, firstly, an engine simulation structure was developed by combining Wang's and Zhai's engine simulation model which was shown in Figure 6.a with a throttle body dynamic model. Then, the developed engine structure was utilized entire modules of intake manifold dynamics rather than manifold pressure and temperature dynamics as shown in Figure 8.a [Nekooei, et.al, 2015]. The new engine model was written based on the Matlab /Simulink functions rather than toolboxes.

JOMAse | Received: xxx | Accepted: xxx | [(42) 1: 1-18]
Published by International Society of Ocean, Mechanical and Aerospace Scientists and Engineers, www.isomase.org., ISSN: 2354-7065 & e-ISSN: 2527-6085

Using the engine structure was previous proposed engine [Nekooei, et.al, 2015] as shown in Figure 8.a, the authors utilized by introducing fuel injection dynamics and crankshaft dynamics as shown in Figure 8.b and Figure 11 which called Proposed New Engine Structure "Nekooei-Koto". In other word, the model was developed based on Wang's engine simulation model by introducing a throttle body dynamic model and utilized the manifold pressure and temperature dynamics.

The Nekooei-Koto's engine model of simulation incorporates three input variables (red break line) as follows:

1. Throttle angle (α),
2. Engine speed (N),
3. Injection fuel rate ($\dot{m}_{fi}$).

The new engine model has two outputs variables (blue break line) as follows:

1. A/F ratio
2. Torque of engine.

The model used an intake manifold dynamics instead of manifold pressure. This new simulation model included three input variables: throttle angle (α), engine speed (N), injection fuel rate ($\dot{m}_{fi}$) based on the injection time and two output variables: AFR and engine torque.

As shown in figure 8.a, there are five main modules for the engine operation as follows:

1. Model of throttle body
2. Model of intake manifold dynamic
3. Model of fuel injection dynamic
4. Model of crank shaft or torque dynamic
5. Model of engine air to fuel ratio (AFR)

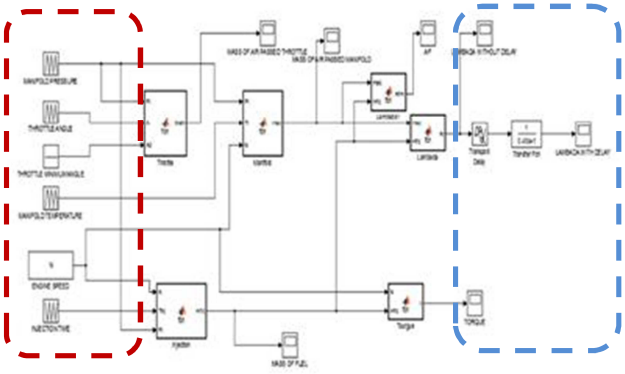

Figure 8.a: Development of new engine simulation structure by Nekooei,et.al, 2015.

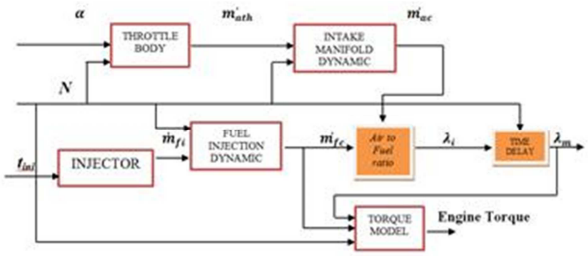

Figure 8.b: Proposed new engine simulation structure [Nekooei, 2013].

4.0 REVIEW ENGINE SIMULATION STRUCTURES

Some general features are described in the simulation models mentioned in section 2.0. It founded that the models can be separated into three parts as follows:

1. Compute the mass of air in cylinder,
2. Calculate the mass of fuel in the cylinder
3. Analyze engine speed or torque.

Alternatively, the calculation of AFR model was based on the outcomes of part 1 and part 2 as mention above. Different characteristics between the models can be included. For example, exhaust pipe dynamics were considered in Alippi's simulation model [Alippi, et.al, 1988 & 2003]. The intake air temperature was simulated in Wang's model [Wang, et.al 2006 & 2008]. The influence of sparking time and throttle dynamics were included in Yoon's model, 2000. Powell's simulation model [Cook, et.al, 1988] was the only model in which a block for the exhaust gas recirculation system was included.

Table 1 is comparison between new and existing engine MVEM. The Table 1 shows that all the dynamic engine parts can be simulated using Wang's [Wang, et.al 2006 & 2008] and Zhai's, et.al, 2010 engine simulation models however without taking account throttle body. However, Yang Bai and Nekooei-Koto engine structure contain all variables of dynamic engine structures, but they are different in fundamental basis as follows:

1. Flow diagram of Nekooei-Koto engine simulation structure as shown in Figure 8.b is not similar to the Yang Bai's engine structure as shown in Figure 7.a.
2. All dynamic equations as shown in section 5.0 defined by Nekooei-Koto are different compared to Yang Bai model p.40 ~ 61 [Bai, 2014].
3. Wall-wetting dynamics in Nokooei model was defined into the fuel injection dynamics based on the equations of 5.9 to 5.15 but in Yang Bai model was based on Equations 3.22 ~ 3.30, p.49 ~ 52 [Bai, 2014].
4. Injector parameter (k) in Nekooei-Koto engine model was obtained by experiment, but in Yang Bai model k was obtained based on Guzella & Onder method (Equation 3.27 p.51) [Bai, 2014]. This seems not proper way to measure the injector parameter (k).
5. Nekooei model for fuel film parameter used equations 5.10 to 5.14 was based on the engine manifold pressure (p_i) and engine speed (N) but Yang Bai engine model was based on the density of fuel, area of fuel evaporation and dimension of intake port.
6. Nokooei-Koto engine model has value of absorbed load as an extra input which was taken from the experiment.
7. Nekooei-Koto model used Gnanam et al., 2006 method to calculate volumetric efficiency which depends on engine speed, but Yang Bai used Hendricks et.al 1996 without taken into account engine speed.
8. Nokooei-Koto engine model is based on the Matlab/Simulink functions but Yang Bai model is based on the Matlab/Simulink tool boxes. In Matlab functions, all parameters can be defined exactly without extra calculation but in tool boxes the users must calculate some parameters at first and then insert them in to the tool boxes, therefore when

JOMAse | Received: xxx | Accepted: xxx | [(42) 1: 1-18]
Published by International Society of Ocean, Mechanical and Aerospace Scientists and Engineers, www.isomase.org., ISSN: 2354-7065 & e-ISSN: 2527-6085

the users have a nonlinear system (SI engines) it is not easy and exact way to calculate many of parameters theoretically, because of that the Matlab tool boxes are not suggested to model of real time engines.

Table 1: Summarized the reviewed engine Mean Value Engine Model (MVEM) Model structures.

Model	Air Mass inside the Cylinder	Fuel Mass inside the Cylinder	Engine Speed	Engine Toque	AFR	Throttle Dynamic	Injection Time	Throttle Angle	Intake Manifold Temperature	Intake Manifold Pressure	Time Delay
Alippi et al. (1998) [2]	√	√	√		√		√	√	√		
Wang (2008) [35] Zhai (2010) [40]	√	√	√		√			√	√	√	√
Yoon et al. (2000) [38]	√	√	√	√	√	√		√			√
Cook and Powell (1988) [13]	√	√		√		√		√		√	
Yang Bai, (2013) [37]	√	√	√	√	√	√	√	√	√	√	√
Nekooei-Koto	√	√	√	√	√	√	√	√	√	√	√

5.0 MATHEMATICAL MODEL

5.1 Model of Throttle Body

In a gasoline engine, the amount of air entering the engine is directly controlled by the throttle. The throttle parameters were the diameter of throttle bore (D) and the diameter of the throttle lot (d). Figure 9 shows the throttle body from a Peugeot 405 1.8i engine. Location of the throttle body is normally between the air filter box and the intake manifold. The task of this valve is to indirectly control the charge ($fuel + air$) to be burned in each cycle. The fuel-air ratio is maintained at a constant level by the fuel-injector or carburetor. A controlling driver is used in a motor vehicle to regulate power. "Throttle pedal," and "accelerator" are other names for this controlling driver.

Figure 9: Throttle body in Peugeot 405 1.8i engine.

Normally, the throttle is a butterfly valve. This valve is installed at the entry of the intake manifold in fuel-injection engine. It is sometimes housed in the throttle body or it can be found in the carburetor in a carbureted engine.

In the simulation model, the air mass flow rate into the intake manifold is calculated by the block of throttle body. Studies conducted by Scattolini et al, 1997 and Yoon et al. 2000 demonstrated that the flow rate equation for the throttle is based on the throttle angle as well as intake manifold pressure.

5.1.1 Air Flow

For the internal combustion in gasoline engines to occur, air is a vital compound. Engine performance system including engine power, torque, speed and emissions, is directly impacted by air flow.

5.1.2 Area of Throttle

The filter and intake are separated by the throttle plate, which is a valve allows for air flow. Air is allowed to flow into the intake manifold by the throttle provided flow area. Heywood's research in 1998 demonstrated that the throttle angle can influence the flow area as shown in Equation 5.1.

$$A_{th}(\alpha) = \frac{\pi D^2}{4}\left(1 - \frac{\cos\alpha}{\cos\alpha_0}\right) + \frac{D^2}{2}\left\{\frac{K}{\cos\alpha}(\cos^2\alpha - K^2\cos^2\alpha_0)^{\frac{1}{2}} - \frac{\cos\alpha}{\cos\alpha_0}\sin^{-1}\left(\frac{K\cos\alpha_0}{\cos\alpha}\right) - K(1-K^2)^{\frac{1}{2}} + \sin^{-1}K\right\} \quad (5.1)$$

Where:

$K = d/D$

and α , α_0, D, d and $A_{th}(\alpha)$ denoted the throttle angle , angle for

JOMAse | Received: xxx | Accepted: xxx | [(42) 1: 1-18]
Published by International Society of Ocean, Mechanical and Aerospace Scientists and Engineers, www.isomase.org., ISSN: 2354-7065 & e-ISSN: 2527-6085

minimum leakage area, Diameter of throttle bore, Diameter of throttle lot and Area of throttle, respectively.

5.1.3 Air Mass Posterior to Throttle

By opening the throttle plate, air trapped before the throttle can move into the intake manifold. Ebrahimi et al, 2012 used a differential equation to calculate the volume of air that moves into the intake manifold. There are several parameters that must be determined before the air flow rate can be calculated. These parameters are the discharge coefficient, the area of the throttle, pressure and temperature before the throttle, pressure of the intake manifold, gas constant, and the specific heat ratio. The relationship between these parameters is shown in Equation 5.2.

$$\dot{m}_{ath} = \frac{C_d A_{th} p_0}{\sqrt{RT_0}} \left(\frac{2\gamma}{\gamma-1}\right)^{\frac{1}{2}} \left[\left(\frac{p_i}{p_0}\right)^{\frac{2}{\gamma}} - \left(\frac{p_i}{p_0}\right)^{\frac{(\gamma+1)}{\gamma}}\right]^{1/2} \tag{5.2}$$

Where; c_d , p_0, T_0 ,R , γ, and p_i denoted the Discharge coefficient ($0 \leftrightarrow 1$), pressure before throttle, temperature before throttle (kelvin), Gas constant *(0.*287 KJ*/(*kg $*$ K*))*, Specific heat ratio and Intake manifold pressure (Kpa).

A linear regression was used in this study as suggested in a study conducted by Andersson, 2005 that established the equation for the dynamic discharge coefficient. A third-order polynomial can describe in equation 5.3.

$$C_d(p_0 , p_i) = -1.47 \left(\frac{p_i}{p_0}\right)^3 + 1.06 \left(\frac{p_i}{p_0}\right)^2 - 0.21 \left(\frac{p_i}{p_0}\right) + 1.01. \tag{5.3}$$

It is worth pointing out that the dynamic behavior of the air passing through the throttle is not clearly represented in the current literature. As shown in Equation 5.3, this discharge coefficient is now explicitly defined by our study.

According to Heywood's study, 1998, in a four-stroke engine, volumetric efficiency (η_v) is a vital parameter. It can be described as a ratio between the real flow of air into the cylinder and the flow of air used from a theoretical volume. Gnanam et al., 2006 stated that preferably, there are some parameters involved in the volumetric efficiency. In an ideal world, η_v is described based on air mass and engine speed.

$$\eta_v = (24.5 \,.\, N - 3.14 \,.\, 10^4) m_a^2 + (-0.167 \,.\, N + 222) m_a + (8.1 \,.\, 10^{-4} . N + 0.352). \tag{5.4}$$

Where; N *and* m_a denoted the engine speed and mass of air (m_a) can be expresses by Equation 5.5.

$$m_a = \frac{M_a \, p_i V_m}{R \,.T_i} \tag{5.5}$$

Where M_a , V_m*and* T_i denoted the air molecular mass kg/kmol, manifold volume and temperature of intake manifold (Kelvin).

5.2. Model of Intake Manifold Dynamic

The intake manifold is the part of an engine that supplies the fuel/air mixture to the cylinders which has faction to evenly distribute the combustion mixture to each intake port in the cylinder head. Figure 10 provides a schematic view of an intake manifold.

The studies conducted by Hendricks et al, 1996, Pieper, et.al, 1999, Yoon et al, 2000, Hashimoto et al. 2006, Wang, et al, 2006, Ceviz, et.al, 2007, Ceviz, et.al, 2010 demonstrated that the rate of the air flow through the throttle and into the intake manifold was defined and related to three parameters. They are throttle angle, atmospheric pressure, and intake manifold pressure. For the SI engine, an air charge per stroke has more important meanings than the normalized air charge during the process of the development of the engine model due to operation is based on the engine events Yoon, et.al, 2000.

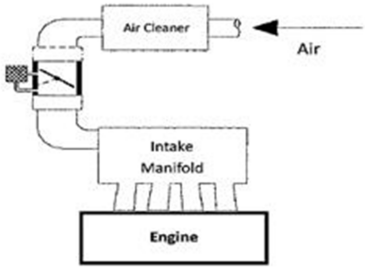

Figure 10: Intake Manifold Schematic [Hendricks et al, 1996]

The amount of air that passes into a cylinder is impacted by intake manifold density, ρ_{ai}. This parameter is expressed in Equations 5.6 and 5.7.

$$\rho_{ai} = \frac{p_i}{RT_i} \tag{5.6}$$

Where;

$$\dot{p}_\iota = \frac{RT_i}{V_m} \dot{m_{at}} - \frac{\eta_v N V_d p_i}{120 V_m} \tag{5.7}$$

Equations (5.2), (5.4) and (5.7) demonstrate that the real amount of air passing into the cylinder $\dot{m}_{ac}$ can be calculated using Equation 5.8.

$$\dot{m}_{ac} = \frac{\eta_v N V_d \rho_{ai}}{2(60)} \tag{5.8}$$

Where; V_d is displacement volume (m^3).

5.3 Model of Fuel Injection Dynamic

Movement of the fuel is via the solenoid valve of injection. This valve is electrically controlled by injection signal into an SI engine. In this engine, various systems of fuel injection and different positions of inject may lead to various outcomes [18]. Model of injection dynamic is mainly a system of fuel delivery in simulating the engine. In this model, by using the air/fuel control system, it is possible to determine the fuel amount which is injected into the intake manifold. This can be declared as a function of injection time and diameter of fuel spray nozzle [Suh, et.al, 2009]

An electrically controlled electromechanical device used for activating a solenoid valve is called a fuel injector. The amount of fuel injected into the intake manifold is calculated using Equation 5.9.

JOMAse | Received: xxx | Accepted: xxx | [(42) 1: 1-18]
Published by International Society of Ocean, Mechanical and Aerospace Scientists and Engineers, www.isomase.org., ISSN: 2354-7065 & e-ISSN: 2527-6085

$$\dot{m}_{fi} = \frac{N}{2} k\left(t_{inj} - t_0\right) \quad (5.9)$$

Since each cycle is equals to two crankshaft rotations, 1/2 factor was presented in the above equation.

Each dynamic part has one or more mathematical equations. In many of equations are many parameters which they have to calculate theoretically or experimentally as example wall-wetting dynamics. In Equation 5.9, k is the injector parameter that introduces how much fuel, in milligrams, will be injected into the manifold per millisecond and it should obtain by an experiment for every type of injector. To measure the value of k the injector nozzle of Peugeot 405 1.8i engine, injector tester has been installed. The injector tester pressure is up to 280 K_{pa}, which the same pressure for the engine fuel pump has been set and then the tester for 40 seconds has been run. The amount of fuel injected into the injector tester glass cylinder has been measured. The amount of fuel injected in one millisecond using the normal calculation has been found. It was $0.71\ x\ 10^{-3}\ grm/ms$.

Since the injected time (t_{inj})or fuel pulse modulation width is commanded by the ECU, it is considered a dynamic parameter in Equation (5.9). According to a study conducted by Chang, et al, 1993 & 1995, a mechanical delay is represented by the solenoid response time (t_0). This delay has a small constant value of 0.41 ms. The dynamic process of fueling was started right after the fuel was injected [Chang, et al, 1995].

The simplest fuel-film-flow model is described by Equation 5.10.

$$\dot{m}_{ff} = \frac{1}{\tau_f}\left(-\dot{m}_{ff} \dot{+} X_f \dot{m}_{fi}\right) \quad (5.10)$$

$$\dot{m}_{fv} = \left(1 - X_f\right)\dot{m}_{fi} \quad (5.11)$$

$$\dot{m}_{fc} = \dot{m}_{fv} + \dot{m}_{ff} \quad (5.12)$$

The fuel flow dynamics in a manifold injection engine is represented in this model. In this model, fuel evaporation occurs in the intake manifold. There are two parameters involved in this model. One is the constant of time for fuel evaporation τ_f and the other one is the fuel proportion, which is placed on the intake manifold or near to the intake valves X_f . They are point dependent parameters and stated based on different conditions of the model as follows:

$$\tau_f(p_i, N) = 1.35(-0.672N + 1.68)(p_i - 0.825)^2 + (-0.06N + 0.15) + 0.56 \quad (5.13)$$

$$X_f(p_i, N) = -0.277\ p_i - 0.055\ N + 0.68 \quad (5.14)$$

It should be noted that model for wall wetting (fuel film parameter) used in the equations 5.10 to 5.14 which it's based on the engine manifold pressure (p_i) and engine speed (N).

Combining Equations 5.10, 5.11 and 5.12 yields:

$$\dot{m}_{fc} = \frac{1+\left(1-X_f\right)s\tau_f}{1+s\tau_f}\dot{m}_{fi} \quad (5.15)$$

5.4 Model of Crank Shaft Dynamic

The system output is the engine torque and it requires that the velocity of the crankshaft is calculated. The operation of the crankshaft system is based on the relationship engine speed and pressure [19]. The velocity of the crankshaft can be calculated using an integral from the consequent torque divided by engine inertia and total torque can be calculated by multiplying the velocity of the crankshaft by engine inertia [Ahmed, et.al, 2011] and can be expressed as:

$$\dot{N} = \frac{1}{J\text{eng}}\ (Tc - T_f - Tp - T_L) \quad (5.16)$$

$$T_{total} = \dot{N}.J\text{eng}$$

Where;

$\dot{N}$: Engine speed
$T\,c$: Combustion torque after sparks
T_f: Friction torque while the piston goes up and down
$T\,p$: Pumping torque
T_L: Load torque
Jeng: Engine inertia

Using the term of pressure or the term of mean effective pressure, the velocity of crankshaft can be expressed as shown in Equation 5.17.

$$\dot{N} = \frac{1}{J\text{eng}}\left[\frac{V_d\left(i_{mep} - tf_{mep}\right)}{4\pi} - T_L\right] \quad (5.17)$$

Where i_{mep} is the net indicated mean effective pressure (IMEP) for a four-stroke engine without a supercharger, and it is a consequence of subtraction between the gross IMEP (g_{mep}) and pumping IMEP (p_{mep}).

$$i_{mep} = g_{mep} - p_{mep} \quad (5.18)$$

The $imep$ can then be computed using Equation 5.19.

$$i_{mep} = \frac{120\eta_f \dot{m}_{fc} Q_{HV} min(\lambda, 1)}{V_d N} \quad (5.19)$$

Where; η_f is the efficiency of the fuel conversion, Q_{HV} is the fuel low heat value, and $\dot{m}_{fc}$ is the fuel flow rate. The type of strongly defines the two first parameters. tf_{mep} is the friction MEP and can be calculated by finding the sum of the mechanical friction MEP (mf_{mep}) and the accessory mean effective pressure (af_{mep}). The tf_{mep} is expressed is Equation 5.20.

$$tf_{mep} = af_{mep} + mf_{mep} \quad (5.20)$$

The effects and variables used for calculating tf_{mep} includes mechanical friction (MEP), which is relative to the friction of journal-bearing, rings and piston, as well as the friction of the valve train. Engine oil viscosity and purity can directly impact journal-bearing friction. The scratch created between the ring pack and piston skirt with the inside wall of the cylinder caused the piston and ring friction. Three different parts are involved in creating the friction for the valve train. They are valve components, pivot rockers, and overhead camshaft. The water and

JOMAse | Received: xxx | Accepted: xxx | [(42) 1: 1-18]
Published by International Society of Ocean, Mechanical and Aerospace Scientists and Engineers, www.isomase.org., ISSN: 2354-7065 & e-ISSN: 2527-6085

oil pumps, together with no charging alternator friction all contribute to MEP. When these effects are combined, it is possible to determine MEP friction base on engine speed as shown in Equation 5.21.

$$tf_{mep} = 0.97 + 0.15\left(\frac{N}{1000}\right) + 0.05\left(\frac{N}{1000}\right)^2 \quad (5.21)$$

Finally, the air flow rate and the fuel flow rate were calculated. The equation for engine speed is provided by Equation 5.22.

$$N = \left[60\left(\int_0^t \dot{N}\, dt\right)\right]/2\pi \quad (5.22)$$

5.5 Model of Engine Air to Fuel Ratio

In SI engines, the AFR is measured by a lambda sensor. The sensor is located in the exhaust manifold and its purpose is to determine how far away from stoichiometry the air-fuel mixture is. To simulate the structure of a lambda sensor (O_2 sensor) and its theory of operation, the dynamic lambda block was used. Some researchers such as Hendricks and Sorenson, 1991,Wagner *et al.*, 2003, Yoon *et al.*, 2000 have demonstrated that it is possible to assume that the dynamic lambda model is a function of two parameters: mass fuel flow and air in the cylinder. It is possible to calculate the lambda input using the following equation:

$$\lambda_i = \frac{A/F}{(A/F)_{Stoich}} \quad (5.24)$$

The actual air to fuel ratio within the cylinder can be described using Equation 5.23.

$$\text{AFR} = \frac{\dot{m}_{ac}}{\dot{m}_{fc}} \quad (5.23)$$

5.6 Time delays

It is important to consider the time delays of injection systems. A time delays in injection systems typically have three causes. Firstly, there could be a delay in the engine between two fuel injection cycles and the expulsion of gases from the exhaust valves. Secondly, there could be a delay in the time that it takes the gases in the exhaust to make contact with the O_2 sensor. Thirdly, the output from the sensor could be delayed. Engine speed significantly effects these delays compared to manifold pressure. Manzie et al., 2001 stated the delays faced by injection systems can be represented by Equation 5.25

$$\lambda_m = \frac{\lambda_i e^{-t_d s}}{t_s s+1} \quad (5.24)$$

Note that s is a complicated variable, which is written in frequency domain fashion, t_s is equal to the O_2 sensor time constant, and t_d is the delay between the exhaust gas reaching the O_2 sensor and the injection point as expressed by Equation 5.25.

$$t_d = \frac{120}{N} \quad (5.25)$$

6.0 SIMULATION OF ENGINE STRUCTURE

The development and confirmation of the engine simulation model implemented using Matlab/Simulink. This model would be used for designing and optimizing the control systems of the engine. There are several reasons for developing a Simulink engine dynamic simulation model. The engine simulation model should be compiled according to the results of the engine dynamic equation together with the parameter data from the model obtained from the engine testing platform. Finally, the model must be verified by comparing the simulation data with data from the experiments.

User-defined functions from the Matlab/Simulnik library have been selected and then the codes for each engine model subsystem have been entered as shown in Figure 11. The red and blue break lines are input and output variables, respectively. This because in Matlab functions (all parameters can be exactly defined without extra calculation but in tool boxes we must calculate some parameters at first and then insert them in to the tool boxes) when there is a nonlinear system of engine (SI engines) it is not easy and exact way to calculate many of parameters theoretically, because of that the Matlab tool boxes were not suggested to be modeling of real time engines.

JOMAse | Received: xxx | Accepted: xxx | [(42) 1: 1-18]
Published by International Society of Ocean, Mechanical and Aerospace Scientists and Engineers, www.isomase.org., ISSN: 2354-7065 & e-ISSN: 2527-6085

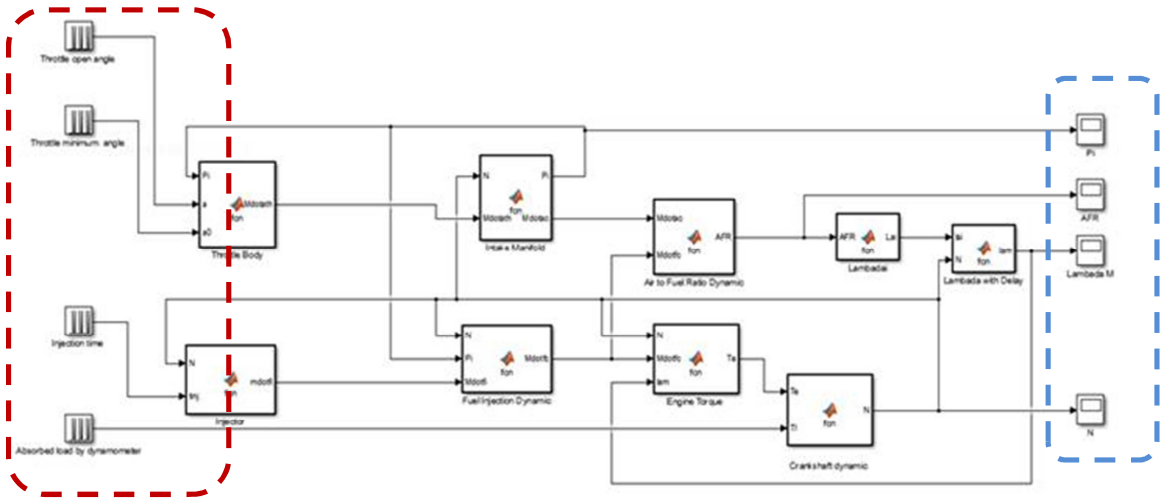

Figure 11: Simulated Engine Model in Matlab/Simulink.

6.1 Model of Throttle Body

As shown in Figure 14 and according to Equation (5.1) and the equations related to Equation (5.2) the air flow rate for the throttle is generated based on the function of throttle open angel and manifold pressure.

Figure 12 shows the structure of the throttle model. The open angle for the throttle depends on the driving mode which is presented at the input subsystem. For instance, when the driver push the gas pedal from the linkage the throttle, the angle will change causing the throttle air flow rate to increase.

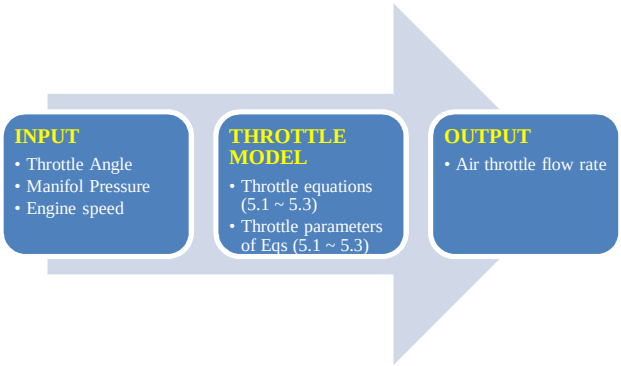

Figure 12: Throttle model structure

Parameters of Equations 5.1 to 5.3 in the throttle model are:

1. Throttle area
2. Throttle plate angle
3. Pressure before the throttle
4. Temperature before the throttle
5. Discharge coefficient
6. Constant of Gas (0.287058 kJ/(kg ∗ K))
7. Intake manifold pressure
8. Specific heat ratio
9. Diameter of the throttle bore
10. Diameter of the throttle shaft

6.2 Model of Intake Manifold Dynamics

When air is delivered from the throttle body to the intake manifold, the flow rate will be affected by the pipe bend. This will result in pressure changes on both sides of the intake manifold. However, the model of the intake manifold dynamics will only be able to compute the pressure and flow rate at the end of the intake manifold. Equations 5.6 to 5.8 reveal that in the intake manifold model, engine speed and air mass after the throttle are input factors. Figure 15 describes the structure of the intake manifold model [19].

As shown in Figure 13, the air flow rate for the throttle can be found using the throttle body model. Furthermore, the density of the intake manifold, manifold volume and volumetric efficiency are the parameters of intake manifold that can be calculated.

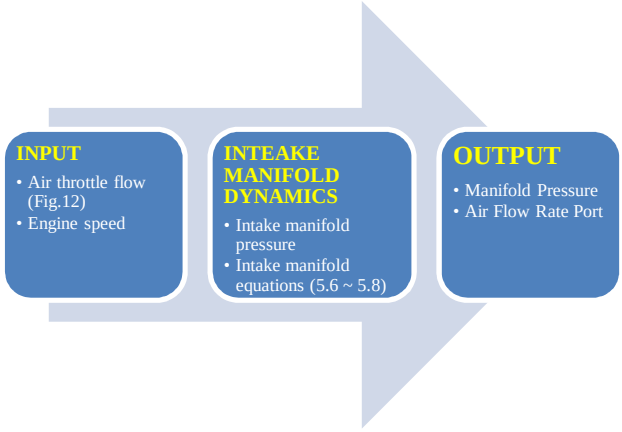

Figure 13: Intake manifold structure

6.3 Fuel Injection Dynamics Model

Fuel is injected when the injection system receives the pulse width modulation signal sent by the ECU. The pulse width modulation (PWM) is based on feedback from the O_2 sensor. The ECU determines how far away the AFR is from stoichiometry AFR (14.6). Next, fuel flows under high pressure via a small nozzle, and the fuel will be atomized by the injection by

JOMAse | Received: xxx | Accepted: xxx | [(42) 1: 1-18]
Published by International Society of Ocean, Mechanical and Aerospace Scientists and Engineers, www.isomase.org., ISSN: 2354-7065 & e-ISSN: 2527-6085

forcefully pumping it into the cylinder or intake port. Thus, as shown in Figure 14, the structure of the model for fuel delivery can be designed to include the injection time and fuel injector time delays as input parameters and the flow rate of the fuel into the cylinder as the output.

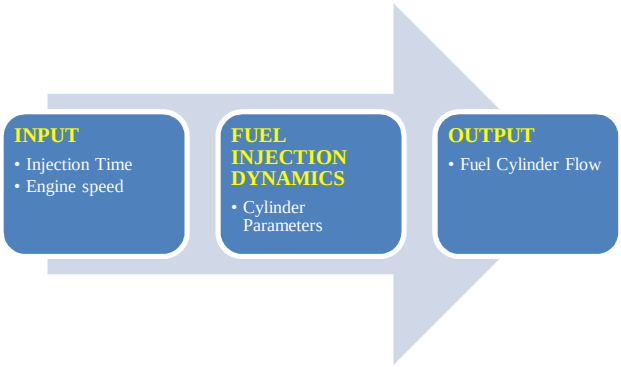

Figure 14: Injection dynamic structure

6.4. Torque Production Model

The combustion process in the cylinder produces engine torque, and the quantity of the torque produced is influenced by the AFR of the mixture in the cylinder, spark timing, and combustion efficiency [38]. The torque model is based on several sub-models such as combustion, friction, load and pumping torques. Torque is based on the conservation of rotational energy by the crankshaft. From the analysis of Equation (5.16) to (5.22), it can be deduced that engine torque is dependent on the variation of speed and effective inertia of the engine or by using the term of pressure or the term of MEP. The engine torque module structure of the engine model is illustrated in Figure 15:

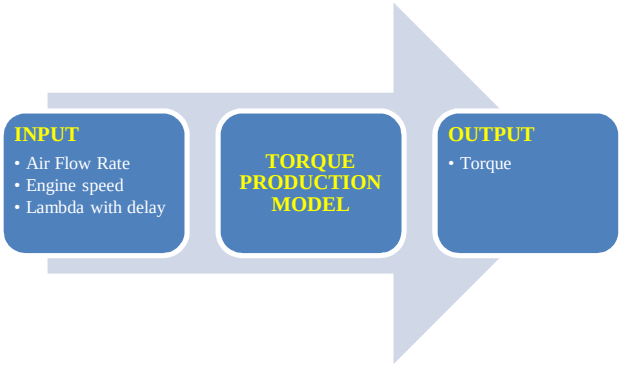

Figure 15: Torque production structure

6.5 Air to Fuel Ratio Dynamic Model with Transport Delay

In SI engines, the AFR is calculated using an O_2 sensor (sometimes known as lambda sensor), which is positioned within the exhaust manifold. This sensor mainly aims at determining the distance between stoichiometry and the air-fuel mixture. The distinctive position of O_2 sensor contributes to reduction of the response time between the fuel injector and the sensor. This time is a significant time delay that is taken into consideration for AFR feedback control systems.

A vital part in the development of the AFR and engine control system was the simulation of the lambda dynamic. The combustion state and the simulation of exhaust was not easily achieved. The amount of air in the cylinder divided by the amount of fuel in the cylinder forms the block of the lambda dynamic simulation (Equations 5.22 to 5.24). The structure of the model of lambda dynamics is illustrated in Figure 16.

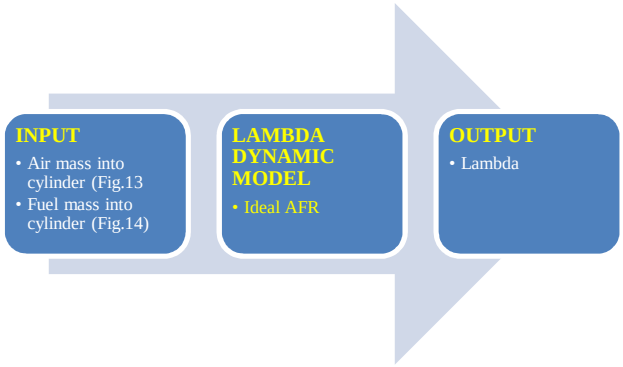

Figure 16: Lambda dynamic structure

To increase the accuracy of simulation, it was necessary to include a reasonable delay in the timing for the of lambda signal before feeding it into the control model. Figure 17 shows the block structure for the simulation

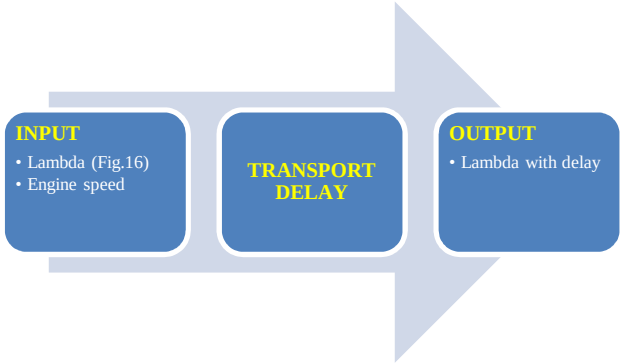

Figure 17: Lambda delay structure

6.6 Air to Fuel Ratio Comparison

Six different types of control methods for controlling AFR from studies conducted by other researchers used for comparison purposes. They are Neural Networks (NN) method, a Sliding Mode Control (SMC) method, a PI control method, Model Predictive Control (MPC) method, Diagonal Recurrent Neural Network (DRNN)-based MPC method and Hybrid Fuzzy Logic Control (HFLC) method.

The air–fuel ratio control result of the MPC controller is shown in the Figure 18 in which the maximum AFR at 16.20 and minimum AFR at 14.05 (red break line). The system output under the developed DRNN-based MPC is displayed in Figure 18. It shows that the maximum AFR at 17.70 and minimum AFR at 13.25 (red break line). Zhai et.al in 2010, also conducted AFR simulation using traditional PI control as shown in Figure 19 with maximum AFR at 22.50 and minimum AFR at 12.80 (red break

JOMAse | Received: xxx | Accepted: xxx | [(42) 1: 1-18]
Published by International Society of Ocean, Mechanical and Aerospace Scientists and Engineers, www.isomase.org., ISSN: 2354-7065 & e-ISSN: 2527-6085

line).

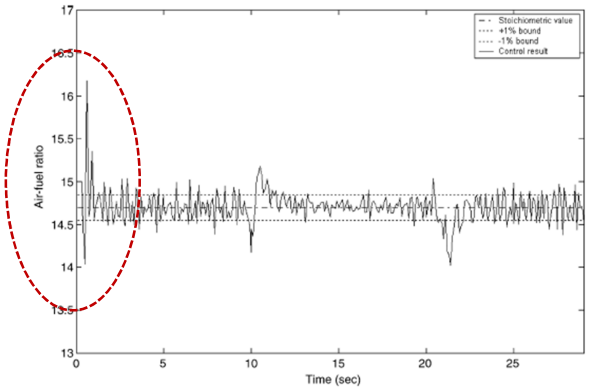

Figure 18: Air–fuel ratio control result of the MPC controller (tracking MAE =v0:2566) [Wang, et.al, 2006].

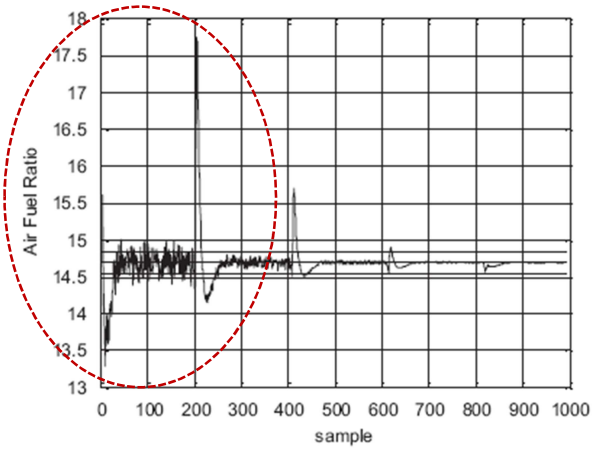

Figure 19: Simulation result of DRNN-based MPC on AFR [Zhai, et.al, 2010].

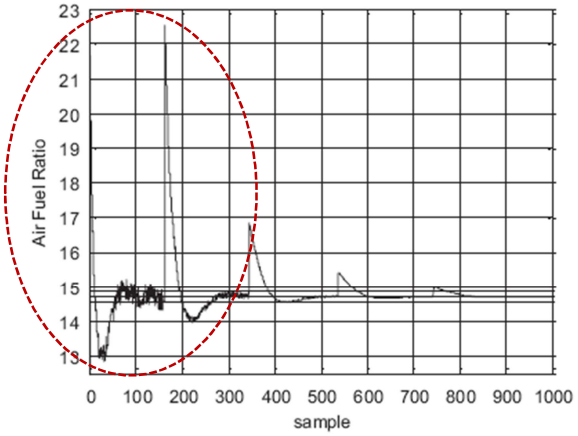

Figure 20: Simulation result of PI control on AFR [Zhai, et.al, 2010].

Yang Bai, 2014 had conducted the test with constant engine load torque which was set at 80 Nm, and the throttle open angle use small value opening as shown in Figure 21.a, the controlled AFR comparison results are shown in Figure 21.b. After 3 seconds, the system is unstable due to the throttle change, and it can be seen that the NN controlled AFR reduced the maximum error by 50% and 30% from the PID control fuzzy PID control.

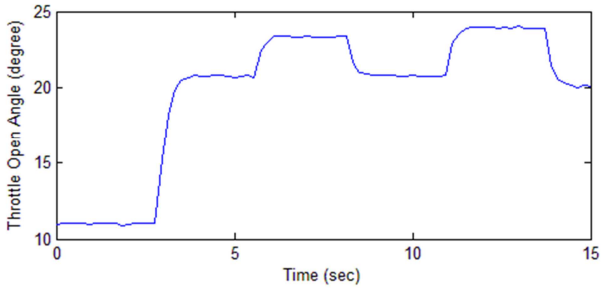

Figure 21.a: Small value throttle open angle input profile [Bai, 2014]

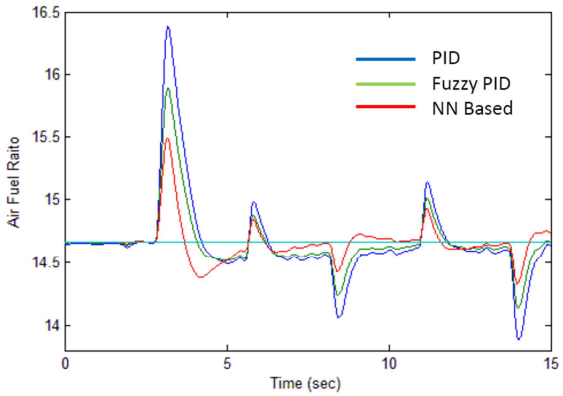

Figure 21.b: AFR Comparison for the constant engine load torque at 80 Nm [Bai, 2014]

In this study, the experiment was conducted using engine of Peugeot 405 1.8i with constant load 40, 50 and 60 Nm. Using the proposed engine model, simulation was carried out using Hybrid Fuzzy Logic Control (HFLC), Developed PID and Convectional Lookup-Table Controller to calculated the AFR. Simulation result at 60 Nm constant engine load was presented at Figures 22 and 23.

JOMAse | Received: xxx | Accepted: xxx | [(42) 1: 1-18]
Published by International Society of Ocean, Mechanical and Aerospace Scientists and Engineers, www.isomase.org., ISSN: 2354-7065 & e-ISSN: 2527-6085

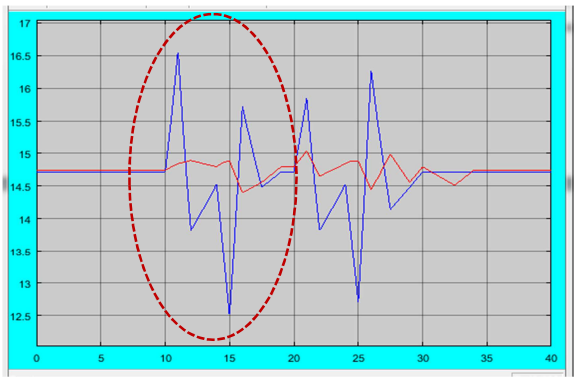

Figure 22: Comparing HFLC with the Developed PID AFR Controller at 60 Nm of constant load.

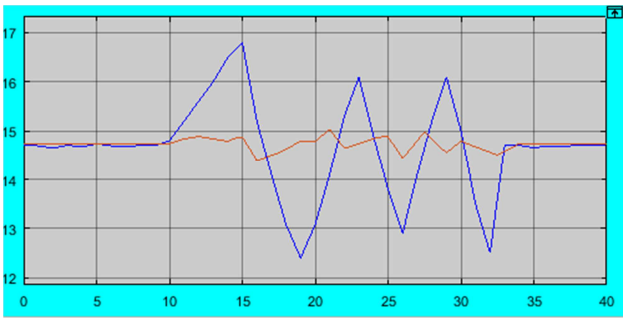

Figure 23: Comparing HFLC with Real tested Engine AFR with Convectional Lookup-Table Controller at 60 Nm Constant Load

In Table 2, the results of a comparison study between an AFR control using Neural Networks (NN) method as shown in Figure 18, a sliding mode control (SMC) method, a PI control method as shown in Figure 19, MPC as shown in Figure 20 and developed HFLC method as shown in Figure 21 are presented. Table 6 shows Comparison between the AFR results for the developed HFLC with NN, SMC, MPC and PI Controller.

Table 2 showed that, the developed HFLC can control the AFR very good in comparison with other methods as mention above. The average error between the maximum and minimum AFR with stoichiometric AFR was just approximately 7 % .The control methods have been reviewed in the Table 6 also controlled the AFR but still there is too big deviation between the AFR and stoichiometric AFR.

Table 2: Comparison Between the AFR results for the developed HFLC with NN, SMC, MPC and PI Controller.

No	Methods	Maximum AFR	Minimum AFR
1	SMC [Pieper, et. al, 1999]	17.64	11.76
2	MPC (Figure 18) [Wang, et.al, 2006]	16.20	14.05
3	DRNN-based MPC (Figure 19) [Zhai, et. al, 2010]	17.70	13.25
	PI (Figure 20) [Zhai, et.al, 2010]	22.50	12.80
5	PID (Figure 21.b) [Bai, 2014]	16.40	13.80
6	Fuzzy PID (Figure 21.b) [Bai, 2014]	15.90	14.10
7	NN (IP) (Figure 21.b) [Bai, 2014]	15.50	14.30
8	Developed PID (Figure 22) Nekooei & Koto	16.50	12.50
9	Convectional Look-up (Figure 23) Nekooei & Koto	16.80	12.40
10	HFLC (Figures 22 & 23) Nekooei & Koto	15.02	14.40

7.0 CONCLUSION

Review on existing engine models has been carried out based on MVEM input parameters as follows: air mass inside the cylinder, fuel mass inside the cylinder, engine speed, engine toque, AFR, throttle dynamic, injection time, throttle angle, intake manifold temperature, intake manifold pressure time delay. It found that all existing engine structures do not use all of the MEVM input parameters dynamic except engine proposed by Yang Bai, 2014. The new simulation engine model was developed using all MVEM input parameters by combining Wang's [35 & 36] and Zhai's, 2010 engine simulation models. This model is exceptionally competent structure to utilizing in engine parameters controlling, for example, AFR and torque. The simulation results were also compared on AFR results using Neural Networks (NN) method, a Sliding Mode Control (SMC) method, a PI control method, Model Predictive Control (MPC) method and Diagonal Recurrent Neural Network (DRNN)-based MPC method. The simulated engine model in Matlab/Simulink showed that AFR using new engine simulation close to the stoichiometric value of 14.7.

ACKNOWLEDGEMENTS

The authors would like to convey a great appreciation to Universiti Teknologi Malaysia and Ocean and Aerospace Research Institute, Indonesia for supporting this research.

REFERENCE

1. Ahmed, Q. and Bhatti, A. I, 2011, *Estimating SI engine efficiencies and parameters in second-order sliding modes. Industrial Electronics*, IEEE Transactions on, 58, 4837-4846.
2. Alippi, C., De Russis, C. and Piuri, V, 1988, A fine control of the air-to-fuel ratio with recurrent neural networks. *Instrumentation and Measurement Technology Conference,*

JOMAse | Received: xxx | Accepted: xxx | [(42) 1: 1-18]
Published by International Society of Ocean, Mechanical and Aerospace Scientists and Engineers, www.isomase.org., ISSN: 2354-7065 & e-ISSN: 2527-6085

1998. IMTC/98. Conference Proceedings. IEEE, 1998. IEEE, 924-929.
3. Alippi, C., De Russis, C. and Piuri, V, 2003, *A Neural-Network Based Control Solution to Air-Fuel Ratio Control for Automotive*, IEEE Transactions On Systems, Man, And Cybernetics—Part C: Applications And Reviews, Vol. 33, No. 2, May 2003.
4. Andersson, P, 2005, *Air charge estimation in turbocharged spark ignition engines*, Department of Electrical ngineering, Linköping University.
5. Balluchi, A., Benvenuti, L., Di Benedetto, M., Cardellino, S., Rossi, C. and Sangiovanni-Vincentelli, A, 1999, Hybrid control of the air-fuel ratio in force transients for multi-point injection engines. Decision and Control, 1999. *Proceedings of the 38th IEEE* Conference on, 1999. IEEE, 316-321.
6. Benninger, N.F. and Plapp, G. 1991, Requirements and Performance of Engine Management Systems under Transient Conditions. *SAE Paper 910083*
7. Bosch, 1994, *Automotive Electric/Electronic Systems*. Wallendale, PA: Society of Automotive Engineers, 1994
8. Cassidy Jr, J. F., Athans, M. and Lee, W. H, 1980, *On the design of electronic automotive engine controls using linear quadratic control theory*, Automatic Control, IEEE Transactions on, 25, 901-912.
9. Ceviz, M, 2007, *Intake plenum volume and its influence on the engine performance, cyclic variability and emissions*, Energy Conversion and Management, 48, 961-966.
10. Ceviz, M. and Akın, M, 2010, *Design of a new SI engine intake manifold with variable length plenum*, Energy Conversion and Management, 51, 2239-2244.
11. Chang, C.-F., Fekete, N. P. and Powell, J. D, 1993, Engine air-fuel ratio control using an event-based observer. *SAE Technical Paper*
12. Chang, C.-F., Fekete, N. P., Amstutz, A. and Powell, J. D, 1995, *Air-fuel ratio control in spark-ignition engines using estimation theory*. Control Systems Technology, IEEE Transactions on, 3, 22-31.
13. Cook, J. and Powell, B. K, 1988, *Modeling of an internal combustion engine for control analysis*. Control Systems Magazine, IEEE, 8, 20-26.
14. Ebrahimi, B., Tafreshi, R., Masudi, H., Franchek, M., Mohammadpour, J. and Grigoriadis, K, 2012, *A parameter-varying filtered PID strategy for air–fuel ratio control of spark ignition engines*, Control Engineering Practice, 20, 805-815.
15. Gnanam, G., Sobiesiak, A., Reader, G., & Zhang, C, 2006, *An HCCI engine fuelled with iso-octane and ethanol* (No. 2006-01-3246). SAE Technical Paper
16. Hashimoto, S., Okuda, H., Okada, Y., Adachi, S., Niwa, S. and Kajitani, M, 2006, *An engine control systems design for low emission vehicles by generalized predictive control based on identified model*, Computer Aided Control System Design, 2006 IEEE International Conference on Control Applications, 2006 IEEE International Symposium on Intelligent Control, 2006 IEEE, 2006. IEEE, 2411-2416.
17. Hendricks, E. and Sorenson, S. C, 1991, SI engine controls and mean value engine modelling. *SAE Technical paper*.
18. Hendricks, E., Chevalier, A., Jensen, A., Sorenson, S.C., 1996. Modelling of the intake manifold filling dynamics. *SAE paper 960037*
19. Heywood, J. B, 1988, *Internal combustion engine fundamentals*, Mcgraw-hill New York.
20. Koto, J. and Ikeda, Y. (2002). A Feasibility Study on a Podded Propulsion LNG Tanker in Arun, Indonesia–Osaka, Japan Route. *The Twelfth International Offshore and Polar Engineering Conference*, 2002. International Society of Offshore and Polar Engineers, pp 525 ~ 532.
21. Manzie, C., Palaniswami, M., & Watson, H. (2001). Gaussian networks for fuel injection control. Proceedings of the Institution of Mechanical Engineers, Part D: Journal of Automobile Engineering, 215(10), 1053-1068.
22. Mohammad Javad Nekooei, J. Koto, M.Pauzi Ghani and Zahra Dehghani, 2015, *A New Engine Simulation Structure Model Applied to SI Engine Controlling*, Journal of Ocean, Mechanical and Aerospace -science and engineering-, Vol.22, pp.9-12.
23. Mohammad Javad Nekooei, Jaswar Koto, 2017, *Hybrid Fuzzy Logic Controller in Matlab/Simulink for Controlling AFR of SI Engine*, International Journal of Environmental Research & Clean Energy, Vol.5 (1), pp.11-20, January, 2017.
24. Mohammad Javad Nekooei, Jaswar, Agoes Priyanto and Zahra Dehghani, 2013, A Review on Engine MVEM Models and AFR Control Methods to Developing a New Engine Model and Ziegler Nichols PID Fuzzy controller: Applied to SI Engines, Journal of Applied Sciences Research, 9(13): pages 6710-6725.
25. Mohammad Javad Nekooei, Jaswar, Agoes Priyanto, Zahra Dehghani, 2014, *A Study on Combustion Modelling of Marine Engines Concerning the Cylindrical Pressure*, Journal of Applied Science and Agriculture, 9(8) June 2014, Pages: 39-44
26. Müller, M., Hendricks, E. and Sorenson, S. C, 1998, Mean value modelling of turbocharged spark ignition engines. *SAE Technical Paper*.
27. Nekooei, Mohammad Javad, Jaswar Koto, A.Priyanto, Zahra Dehghani, 2015, *Reviewed on Combustion Modelling of Marine Spark-Ignition Engines*, Journal of Ocean, Mechanical and Aerospace -Science and Engineering-, Vol.17 1 (2015): 1-4.
28. Nekooei, Mohammad Javad, Jaswar Koto, and A. Priyanto, 2014, *Review on Combustion Control of Marine Engine by Fuzzy Logic Control Concerning the Air to Fuel Ratio*, Jurnal Teknologi 66.2.
29. Nekooei, Mohammad Javad, Jaswar Koto, and A. Priyanto, 2015, *A Simple Fuzzy Logic Diagnosis System for Control of Internal Combustion Engines*, Jurnal Teknologi 74.5 (2015).
30. Nekooei, Mohammad Javad, Jaswar Koto, and Agoes Priyanto, 2013. *Designing Fuzzy Backstepping Adaptive Based Fuzzy Estimator Variable Structure Control: Applied to Internal Combustion Engine*, Applied Mechanics and Materials. Vol. 376. 2013.
31. Pieper, J. and Mehrotra, R, 1999, Air/fuel ratio control using sliding mode methods. *American Control Conference*, 1999. Proceedings of the 1999, 1999. IEEE, 1027-1031.
32. Priyanto, Agoes, and Mohammad Javad Nekooei, Jaswar Koto, 2014, *Design Online Artificial Gain Updating Sliding Mode Algorithm: Applied to Internal Combustion Engine*, Applied Mechanics and Materials. Vol. 493. 2014.

33. Scattolini, R., Siviero, C., Mazzucco, M., Ricci, S., Poggio, L. and Rossi, C, 1997, *Modelling and identification of an electromechanical internal combustion engine throttle body*, Control Engineering Practice, 5, 1253-1259.
34. Suh, H., Park, S. and Lee, C, 2009, Effect of grouped-hole nozzle geometry on the improvement of biodiesel fuel atomization characteristics in a compression ignition engine, *Proceedings of the Institution of Mechanical Engineers*, Part D: Journal of Automobile Engineering, 223, 1587-1600
35. Wagner, J.R, Dawson, D.M and Zeyu.L, 2003, *Nonlinear Air-to-Fuel Ratio and Engine Speed Control for Hybrid Vehicles*, IEEE Transactions On Vehicular Technology, Vol. 52, No. 1, January 2003
36. Wang, S and Yu, D, 2008, *Adaptive RBF network for parameter estimation and stable air–fuel ratio control*, Neural Networks, 21, 102-112.
37. Wang, S.W, Gomm, J.B, Page, J.F and Douglas, S.S, 2006, *Adaptive RBF network for parameter estimation and stable air–fuel ratio control*, Engineering Applications of Artificial Intelligence 19 (2006) 189–200.
38. Yang Bai, 2014, *Studies on Si Engine Simulation and Air/Fuel Ratio Control Systems Design*, Ph.D Thesis, School of Engineering and Design, Brunel University, London, United Kingdom, April 2014.
39. Yoon, P., Park, S., Sunwoo, M., Ohm, I. and Yoon, K. J, 2000, Closed-loop control of spark advance and air-fuel ratio in SI engines using cylinder pressure, *SAE Technical Paper*.
40. Zhai, Y.J and Yu, D.L 2009, *Neural network model-based automotive engine air/fuel ratio control and robustness evaluation*, Engineering Applications of Artificial Intelligence 22 (2009) 171–180.
41. Zhai, Y.J, Yu D.W, Guo, H.Y and Yu, D.L 2010, *Robust air/fuel ratio control with adaptive DRNN model and AD tuning*, Engineering Applications of Artificial Intelligence 23 (2010) 283–289.
42. Zhai1, Y.J, Yu, D.L, Reza Tafreshi1, Yasser Al-Hamidi, 2011, *Fast predictive control for air-fuel ratio of SI engines using a nonlinearinternal model*, International Journal of Engineering, Science and TechnologyVol. 3, No. 6, 2011, pp. 1-17.

JOMAse | Received: xxx | Accepted: xxx | [(42) 1: 1-18]
Published by International Society of Ocean, Mechanical and Aerospace Scientists and Engineers, www.isomase.org., ISSN: 2354-7065 & e-ISSN: 2527-6085